Science of the Total Environment 744 (2020) 140745

Contents lists available at ScienceDirect

Science of the Total Environment

journal homepage: www.elsevier.com/locate/scitotenv

Phenomenology and geographical gradients of atmospheric deposition in southwestern Europe: Results from a multi-site monitoring network

Jorge Pey [a,*], Juan Cruz Larrasoaña [b], Noemí Pérez [c], José Carlos Cerro [d,e], Sonia Castillo [f,g], María Luisa Tobar [d], Amalia de Vergara [h], Icíar Vázquez [h], Jesús Reyes [h], María Pilar Mata [h], Tania Mochales [b], José María Orellana [b], Jesús Causapé [b]

[a] ARAID – Instituto Pirenaico de Ecología (CSIC), 50059 Zaragoza, Spain
[b] Instituto Geológico y Minero de España, 50006 Zaragoza, Spain
[c] Instituto de Diagnóstico Ambiental y Estudios del Agua (CSIC), C/Jordi Girona 18-26, 08028 Barcelona, Spain
[d] Laboratory of the Atmosphere, Govern Illes Balears, 07009 Palma de Mallorca, Spain
[e] Laboratory of Environmental Analytical Chemistry, Illes Balears University, 07122 Palma de Mallorca, Spain
[f] Andalusian Institute for Earth System Research (IISTA-CEAMA), 18071 Granada, Spain
[g] Department Applied Physics, University of Granada, 18071 Granada, Spain
[h] Instituto Geológico y Minero de España, 28760 Tres Cantos, Spain

HIGHLIGHTS

- Atmospheric deposition at 15 sites: pristine, agricultural, urban and industrial
- Partitioning of soluble and insoluble deposition
- Geographical gradient from Atlantic to Mediterranean climate in South-Western Europe
- African dust contribution enhanced in the Central Pyrenees
- Large emissions from the semi-arid Ebro-Valley region

GRAPHICAL ABSTRACT

ARTICLE INFO

Article history:
Received 10 April 2020
Received in revised form 25 June 2020
Accepted 2 July 2020
Available online 11 July 2020

Editor: Prof. Pavlos Kassomenos

Keywords:
African dust
Regional resuspension
Urban road dust

ABSTRACT

This article presents the results of atmospheric deposition from a 15-sites network which cover remote, agricultural, urban and industrial areas in the Iberian Peninsula and the Balearic Islands, with the aim of exploring geographical, climatic and natural vs anthropogenic gradients. Annual average fluxes of global deposition, discriminating insoluble (3,5–20,7 g m^{-2} $year^{-1}$) and soluble-inorganic (7,1–45,5 g m^{-2} $year^{-1}$) aerosols are discussed, seasonal patterns are regarded, and an attempt to estimate the impact of the main sources is presented. The wide range of atmospheric deposition fluxes (DF) regarding soluble (DF_{SOL}) and insoluble (DF_{INS}) has been investigated taking into consideration the contribution from nearby to long-distance sources, such as African dust, or regional-to-nearby ones, which include agricultural dust in the Ebro Valley, industrial emissions at different parts, urban dust at all cities, or saline dust resuspension from a dissicated lake bed.
DF_{SOL} is made up of marine aerosols, prevailing in coastal areas, with few exceptions in the Ebro Valley; nitrogen-species, homogeneously distributed across the network, with few exceptions due to agricultural sources; mineral

* Corresponding author.
E-mail address: jorge.pey@ipe.csic.es (J. Pey).

https://doi.org/10.1016/j.scitotenv.2020.140745

Nutrients
Western Mediterranean
Agricultural dust

dust, enhanced in the Ebro Valley owing to regional and agricultural emissions; and phospathe, displaying comparable values to other studies in general, but three hotspots at regional background environments have been identified.
DF_{INS} particles followed the aridity pattern, especially where anthropogenic emissions take place. Our estimates indicate that the regional dust to DF_{INS} in the Ebro Valley represented 23–30%, overpassing 50% at intensive agricultural areas. Similarly, urban-metropolitan contributions accounted for 37–45% at the four cities, and 55% at the industrial one. African dust deposition was enhanced in the Central Pyrenees (75–80%) as a result of the magnification of atmospheric washout processes, and in south-eastern Iberia (69%) owing to the higher frequency of dust outbreaks.

1. Introduction

Once completed their lifetime in the atmosphere, atmospheric aerosols are transferred back to Earth surfaces in which they interact in different ways according to their intrinsic physic and chemical properties, but also depending on the media in which they are deposited. Dry and wet deposition of atmospheric particles and gases are the two mechanisms in which these substances are transferred back to the surface (Seinfeld and Pandis, 2006). Dry deposition is related to mechanisms like inertial impaction, interception, Brownian diffusion or phoretic forces (Seinfeld and Pandis, 2006), and wet deposition involves those particles acting as cloud condensation nuclei (in-cloud scavenging or rainout), and those encountered by raindrops, snowflakes, hails, dripping fog when occurring, or those related to dew processes (bellow-cloud scavenging or washout). The importance of dry versus wet deposition depends on the type of pollutant and their concentrations (coarse aerosol versus fine aerosols and gases) and the type of climate (arid versus humid-temperate). According to Hou et al. (2018), wet scavenging is the key factor for maintaining the balance between the sources and sinks of atmospheric aerosols. However, dry deposition has been found to be relevant for elements associated to coarse aerosols in the Mediterranean region (Markaki et al., 2003; Izquierdo and Àvila, 2012; Morales-Baquero et al., 2013).

The scientific significance of atmospheric deposition studies hinges on their effects on climate and ecosystems. It is well known that atmospheric aerosols are essential drivers of the water cycle. According to physic and chemical characteristics, aerosols may act as cloud condensation nuclei (CCN), allowing cloud formation and favoring the redistribution of water around the Earth. The chemical composition of these CCN and the composition of the particles washed out by rain droplets, hail particles or snowflakes may drive the contamination or the nutrition of certain aquatic ecosystems. For example, the excessive deposition of nitrogen species (nitrates, nitrites or ammonium), in many cases acting as CCN, may cause their acidification or eutrophication (Galloway et al., 2008; Bobbink et al., 2010; EEA, 2013; García-Gómez et al., 2014). More recently, special attention is paid to the darkening effect caused by black carbon or mineral dust deposition on ice and snow surfaces. Such processes is behind important albedo variations (Qu et al., 2014), with the overall modification of the radiative balance at different geographical scales.

Certain geochemical aerosol inputs are essential to maintain biodiversity in several environments worldwide. Actually, Saharan dust, which is transported continuously towards America, is the most important fertilizer of the Amazonia (Yu et al., 2015). Moreover, deposition of mineral dust iron-rich particles provokes algae blooms (Prospero et al., 1996; Zhu et al., 1997; Lenes et al., 2001; Mahowald et al., 2009; Westrich et al., 2016), which is associated either to beneficial effects (e.g. enhancing CO_2 sequestration) or to negative consequences (e.g. eutrophication). On the other hand, the atmospheric deposition of trace metals from anthropogenic origin, which occurs constantly even in the most pristine environments (Bacardit and Camarero, 2010a; Camarero et al., 2009), has been related to negative effects in the marine phytoplankton growth (Jordi et al., 2012).

To deal with these and other impacts, a number of atmospheric deposition surveillance networks are in operation at continental scales. To give some examples, the National Atmospheric Deposition Program of the United States (http://nadp.slh.wisc.edu) is in operation since 1978. In Europe, the European Monitoring and Evaluation Programme (http://www.emep.int/) is performing the surveillance of a number of atmospheric parameters, including atmospheric deposition, at several regional background locations (13 sites in Spain). Besides of these wide-range networks, other observations on atmospheric deposition are available in several regions. In the Mediterranean area, the most recent network was in operation from 2011 to 2013 in order to characterize Saharan dust deposition (Vincent et al., 2016). In northeastern Spain, the Catalan network for rainwater composition, lead by the Departament de Territori i Sostenibilitat, is devoted to the measurement of nitrogen components, and their results have been summarized in Àvila et al. (2010). Likewise, a long-term monitoring of atmospheric deposition, coupled with detailed analytical determinations and source identification, is being conducted since the 80's at the Montseny Natural Park, a regional background area 40 Km northwards of Barcelona (Àvila, 1996; Àvila and Peñuelas, 1999; Àvila and Rodà, 1991, 2012; Izquierdo et al., 2012, 2014; Castillo et al., 2017). Northwards of Montseny, in the Central Pyrenees, a number of other detailed studies have been performed (Appleby et al., 2002; Bacardit and Camarero, 2009, 2010a, 2010b; Camarero et al., 2009). Likewise, a number of short-term atmospheric deposition observations performed near to atmospheric pollution hotspots are available from other regions in Spain (Alastuey et al., 1999; Castillo et al., 2013a, 2013b; Fernández-Olmo et al., 2015; Morales-Baquero et al., 2006, 2013; Rodriguez-Navarro et al., 2018; or Torres-Sánchez et al., 2019, among others). In all these cases, fluxes of atmospheric nutrients and certain toxic pollutants have been monitored, in some cases during decades (Avila et al., 2020). Despite these efforts, there is a lack of comprehensive studies at the pan-regional scale to answer some of the open questions at present. With this aim, the DONAIRE network (named according to the project funding this study) was built to answer some of the open questions by carrying out an integrated study on atmospheric deposition in Northern and Eastern Spain, a vast region in between the Cantabrian and the Mediterranean Seas: 1) *which is the role of topography in deposition fluxes in a region in which altitudinal gradients varying significantly in short distances*; 2) *are there important differences when comparing densely populated areas against quasi-demographic deserts*; 3) *which is the impact of industrial and urban emissions with respect to others in which agriculture and farming prevails in terms of fluxes, composition and ecological effects*; and 4) *are arid regions an important source of atmospheric particles?; 5) which is the distribution of African dust deposition in this region?*. In this article we focus on atmospheric DF as well as on their geographical patterns and phenomenology. Forthcoming articles will provide detailed information regarding magnetic properties; chemical composition and sources; or toxicological effects of the deposited aerosols on soil microbiota.

2. Methodology

2.1. The DONAIRE network

Monitoring sites were placed following a number of criteria: 1) they were located next to meteorological observatories and, when possible,

installed in air quality monitoring stations (8 out of 15 sites); 2) at least two monitoring sites were deployed in every region, one in the main city and another in a representative regional background location; 3) the network had to cover from pristine environments to highly polluted areas such as urban and industrial locations, passing through agricultural regions; and 5) accesibility was to be guaranted throughout most of the year.

The DONAIRE network is dedicated to the monitoring of atmospheric deposition. The initial conception included 12 monitoring sites located in the NE of the Iberian Peninsula and the Balearic Islands, and data collection started in June 2016. Thereafter, other regional background observatories were added: one in the Gallocanta Natural Reserve (an agricultural region southwards of the Ebro Valley), another in a mountain location in the Picos de Europa National Park (located in northern Iberia), and a last one in a small village in southern Spain (Frigiliana, Málaga). Overall, 15 monitoring sites were finally managed (Fig. 1, Table 1, Fig. S1, and the suplementary file "DONAIRE network.kmz").

The DONAIRE network records bulk atmospheric deposition. For this purpose, home-produced collectors were built-up. They consist of a polyethylene funnel (diameters ranging from 260 to 340 mm) acting as the collection surface in which atmospheric deposition befalls; a 10 L polyethylene container; a silicone tube, inserted inside a rigid PVC cylinder, connecting the funnel and the container; and a dark box in which the 10-L containers and part of the tubing connections were sited, necessary to lessen the ocurrence of photosyntetic processes in the accumulated samples (see Fig. S2). The overall size of the collector keep the atmospheric collection surface at least 2 m above the ground, thus minimizing the impact of local resuspension. In most cases, collection surfaces were located at 4 to 5 m above the ground. Eight of the collectors were placed in the roof of air quality monitoring sites (in the four cities, at the industrial site, and in two of the regional background sites) or other buildings (1 regional background site). Details on location, type and sampling intervals of the monitoring sites can be found in Table 1.

At the beginning of the project the monitoring calendar was defined. The objective with the calendar was to coordinate the monitoring program in order to have simultaneous samples at all sites. Sampling frequency was established in 15 days (±2 days) during the first year of measurements (24 samples per year/site). From the second year onwards, sampling frequency was modified to 30 days (12 samples per year/site), coinciding with calendar months. All the results of this work refer to the period June 2016–June2017, except for Frigiliana (September 2016–September 2017) and Gallocanta (August 2017–August 2018). Thus, the results could be considered comparable in all cases with the exception of Gallocanta, in which their annual results are from a different year. Only few comments are referred to longer observations.

2.2. Field work

Field work consisted of: 1) cleaning of the funnel with 500 ml of bi-distilled water by using a plastic brush, integrating the resulting solution in the accumulated sample; and 2) replacement of the containers by new-cleaned ones. In some cases, bi-distilled water was not used (i.e when it was raining). When necessary, funnels, tubes or other elements were replaced by new ones. All these informations were notated and taken into account subsequently. When using bi-distilled water, the small amount of chemicals added by the distilled water, which was regularly analyzed, and the dilution effect caused by their addition was taken into account. Only few samples were missed in the whole campaign: some of them due to vandalism acts; and few of them due to adverse meteorological conditions (composite samples were, therefore, obtained). Overall, data collection ranged from 95 to 100%.

2.3. Laboratory

After field work, samples were stored in dark conditions at 4 °C. The beginning of the sample treatment started with the removal of very large particles such as insects or vegetable debris by using a 100 μm

Fig. 1. Location and type of sites included in the DONAIRE network.

Table 1
Geographical coordinates, elevation above sea level, type of area, sampling period and average annual precipitation of DONAIRE network sites. Annual precipitation values correspond to the records from our collectors: June 2016–June 2017, except in Frigiliana (September 2016–September 2017) and Gallocanta (August 2017–August 2018).

	Latitude	Longitude	Altitude (m a.s.l.)	Type of area	Start date	End date	Annual precipitation
Cantabrian and Pyrenean region							
Enol	43,272	−4,991	1070	Regional	Dec. 2015	ongoing	1286 mm
Orgi	42,960	−1,680	512	Regional	Jun. 2016	Sep. 2018	609 mm
Pamplona	42,800	−1,650	450	Urban	Jun. 2016	Sep. 2018	636 mm
Ordesa	42,650	−0,090	1190	Regional	Jun. 2016	ongoing	1135 mm
Ebro Valley							
Chiprana	41,290	−0,240	156	Regional-industrial	Jun. 2016	ongoing	255 mm
Almudévar	42,020	−0,660	456	Agricultural	Jun. 2016	ongoing	484 mm
Gallocanta	40,995	−1,507	995	Regional	Mar. 2017	ongoing	183 mm
Zaragoza	41,640	−0,890	247	Urban	Jun. 2016	ongoing	316 mm
Monzón	41,920	0,190	279	Industrial	Jun. 2016	Jun. 2017	519 mm
Ejea[a]	42,060	−1,130	336	Agricultural	Jun. 2016	Mar. 2017	370 mm
Mediterranean							
Montseny	41,780	2,350	720	Regional	Jun. 2016	ongoing	867 mm
Barcelona	41,390	2,120	63	Urban	Jun. 2016	ongoing	502 mm
Joan March	39,680	2,690	172	Regional	Jun. 2016	Jun. 2017	544 mm
Palma	39,570	2,660	12	Urban-traffic	Jun. 2016	Jun. 2017	601 mm
Frigiliana	36,792	−3,898	320	Rural	Sep. 2016	ongoing	401 mm

[a] Precipitation data from Ejea for the period March–June 2017 obtained from the nearby meteorological station.

size filter. Before the next step, 47 mm pre-heated quartz fibre filters (PALL tissuquartz 2500QAT-UP) were prepared. Filters were previously kept in controlled conditions (Tª 22–24 °C; RH 25–35%) in a vertical dry-keeper and weighted two times by using an electronic microbalance (4-decimals) in different days. After that, each sample was filtered individually by using a filtration ramp connected to a vacuum pump with up to three positions. Each sample was always entirely filtered. As a result of this process, two or more filters were obtained and the collected water volume was quantified. A 250 ml aliquot of each sample was stored at 4 °C until analysis of soluble inorganic particles, including the most abundant anions (HCO_3^-, NO_3^-, Cl^-, SO_4^{2-}, PO_4^{3-}) and cations (K^+, Na^+, Mg^{2+}, Ca^{2+}, NH_4^+). Likewise, the obtained filters were conditioned and weighted again two times in different days, with an acceptance criteria of inter-weights <1 mg. From filters, the deposition flux (DF) of insoluble particles (DF_{INS}) was obtained, considering the mass difference between the final filters and their respective blanks, and taking into account the collection surface.

2.4. Analytical determinations: anions and cations

All anions except HCO_3^- were determined by using Ion Chromatography (881 Compact IC Pro, Metrohm) and all cations and HCO_3^- were obtained by means of a Continuous Flow Analyzer (Alliance Futura, Alliance Instruments) in the Geological Survey of Spain facilities in Tres Cantos (Madrid). Bi-distilled water used during field work was regularly analyzed and the results were considered for calculations. Thereafter, taking into account the accumulated volume, the collection surface and the concentration of soluble-inorganic species, the related DF of soluble inorganic species (DF_{SOL}) were calculated for each monitoring period. In both cases, reference certified materials and internal and external calibration standards were used in each set of samples. Annual intercomparison exercises are conducted every year (z score < 2). Accuracy and precision for both techniques is 10%. For the Ion Chromatography, a 6-month calibration is conducted and the method is validated once per year.

This information has been clustered as folows: the "marine group" accounts for the totality of Na^+ and Cl^-, and the marine fraction of Mg^{2+} and SO_4^{2-} taking into account the typical molar ratios observed in seawaters (Millero et al., 2008); the "mineral group" includes the entire amount of Ca^{2+}, K^+ and SiO_2, and the remaining content of Mg^{2+}; the "non sea-salt sulfate" considers all the remaining sulfate after removing its marine fraction; the "nitrogen species group" includes all NO_3^-, NO_2^- and NH_4^+; the PO_4^{3-}; and finally the inorganic soluble carbon, which is based on amount of HCO_3^-. The sum of all these clusters constitutes the DF_{SOL}.

2.5. Identification of North-African dust outbreaks and estimation of African dust fluxes

Aeolian dust from North African deserts is transported towards southern Europe regularly. In Spain, dust from North Africa is observed every year between 10 and 35% of the days (Pey et al., 2013a). In this study, the identification of dust episodes has been done as in Pey et al. (2013a) but the impact of dust deposition in the DONAIRE network has been derived from BSC dust deposition maps (http://www.bsc.es/projects/earthscience/visor/dust/med8/dep/archive/). During the period under study, several dust deposition events were observed, some of them of a considerable magnitude.

In order to estimate DF of African dust (AD), $DF_{(AD)}$, two different approaches have been followed:

– Method 1 (M1): annual scale

This method, used to estimate the $DF_{(AD)}$ to soluble and insoluble annual fluxes, is based on this simplified approach.

$$DF = DF_{(no-AD)} + DF_{(AD)}$$

where the $\mathbf{DF_{(no\text{-}AD)}}$ is the accumulated annual value for all periods excepting those affected by African dust, and $\mathbf{DF_{(AD)}}$ is obtained by difference between the **DF** and the $\mathbf{DF_{(no\text{-}AD)}}$.

– Method 2 (M2): 15-days scale

This second method is based on the awareness that the $\mathbf{DF_{(AD)}}$ during certain 15-day periods is included in $\mathbf{DF_{(no\text{-}AD)}}$, where $\mathbf{DF_{(no\text{-}AD)}}$ has been estimated by averaging 15-days periods without AD influence for each site. As a result, for each period under the impact of AD, the overal DF was splitted into two components: 1) one corresponding to $\mathbf{DF_{(no\text{-}AD)}}$, which corresponds to the average of the no AD 15-days episodes; and 2) other associated to the $\mathbf{DF_{(AD)}}$, which results from the subtraction to DF the $DF_{(no\text{-}AD)}$ African dust. This second method is akin to the first one but this has been applied to each individual period, which

allow us to estimate periodic dust inputs, and the former is only feasible to estimate the annual input.

2.6. Meteorological and air quality data

Local meteorological data were obtained from the Spanish Meteorological Agency AEMET and, in few cases, from other sources including local meteorology from the air quality sites. Precipitation data were used with a double purpose: to validate the readings of our home-produced atmospheric deposition devices and to correct some of the data. Details on the comparability of these data are included in the supplementary excel file. Actually, certain extreme rain events overflooded the 10-L containers. In those cases, the precipitation registered in the nearest meteorological station during the monitoring period was used to rebuild the theoretical volume in the container. On the other hand, wind data were used to identify at each site the main wind components in order to better understand the phenomenology at the microscale.

Air quality data (SO_2, NO, NO_2, O_3 and PM_{10}) from regional and local air quality networks (Fig. 1) has been used in this study. Data from those sites are obtained following stardardized protocols and the requirements of the European Air Quality directives to assure the comparability of the data.

3. Results

3.1. Dry versus dry + wet deposition

The DONAIRE network was designed to register bulk atmospheric deposition. According to sampling intervals (around 15 days), most of the obtained samples were the result of a mixture of dry and wet deposition. In spite of this, a significant number of the samples were the result of only dry deposition conditions, when the recorded rain values were bellow 2 mm in the whole period. As shown in Fig. 2, the highest number of samples obtained under dry deposition conditions (period June 2016–July 2017) was recorded in Frigiliana-southern Spain and in the Chiprana-Ebro Valley (42–43% of the periods were entirely dominated by dry conditions). The recurrence and persistence of extended dry periods is reduced towards northern regions, where the number of 15-days dry periods decrease to 30–39% in the Balearic Islands and other parts of the Ebro Valley, 21–29% in the NE Iberian Peninsula, and 15–21% in the Cantabrian-Pyrenean region. Enol and Gallocanta are not included in this analysis owing to their different sampling-frequency intervals. As deduced from Fig. 2, there are two main factors controlling the partitioning between dry/(dry+wet) samples, namely the location of the monitoring site in terms of latitudinal position and its distance to the coastline. Cantabrian-Pyrenean and Mediterranean sites, as well as the periferic ones in the Ebro Valley are perfectly aligned regarding latitudinal position and atmospheric dry-deposition frequency: each degree southwards equals to a 4,5% increase in dry-deposition conditions ($R^2 = 0,85$). On the other hand, sites located in the central part of Ebro Basin behave in a different way. These three sites appear isolated wih respect to the rest, in a drier context.

3.2. Global atmospheric deposition fluxes

In general, annual atmospheric DF at regional background sites display a wide range of variability, from 10,6 g m^{-2} $year^{-1}$ in Orgi to 14,7–19,5 g m^{-2} $year^{-1}$ in Chiprana, Montseny and Hospital Joan March, going up to 26,8–34,5 g m^{-2} in Frigiliana, Ordesa and Enol, and reaching 55,5 g m^{-2} in Gallocanta. Urban sites display annual DF ranging from 16,1 g m^{-2} $year^{-1}$ in Pamplona to 31,0 g m^{-2} $year^{-1}$ in Zaragoza. In Table 2, the monitoring sites are grouped according to their geographical-climatic context.

In the Cantabrian-Pyrenean region there is a wide range of values regarding global DF, from 10,6 to 34,5 g m^{-2} $year^{-1}$ and, depending of the site, driven by the amount of soluble-inorganic species (Enol) or insoluble ones (Ordesa). The variation in the Mediterranean region is moderate (15,2–28,7 g m^{-2} $year^{-1}$) and generally controlled by soluble-inorganic aerosols. In the Ebro Valley region, the global DF range varies from 14,7 to 39,7 g m^{-2} $year^{-1}$, being equally important soluble-inorganic and insoluble particles to explain the observed values. The exception is Gallocanta, which displays extremely high DF highly controlled by soluble-inorganic particles associated to resuspension processes of saline sediments during long drought periods affecting the lake. Overall, atmospheric deposition is enriched in insoluble particles in the Ebro Valley region, Central Pyrenees (Ordesa) and in the southernmost site (Frigiliana), whereas soluble-inorganic contributions prevail in coastal areas and adjacent regions.

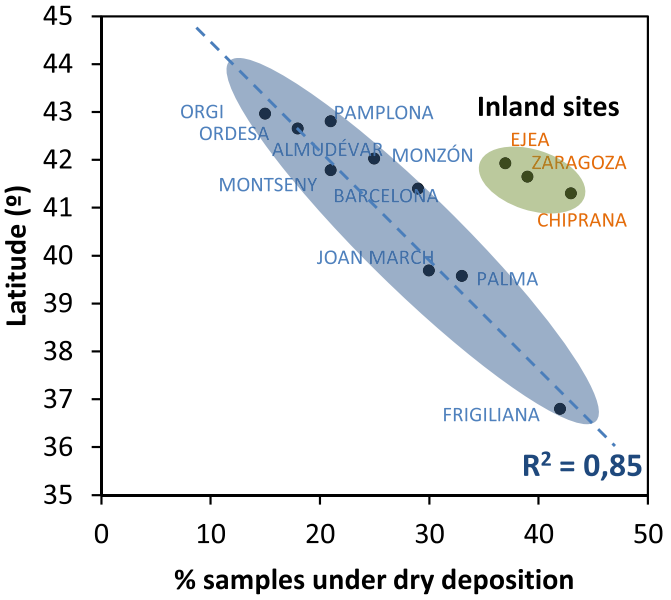

Fig. 2. Relation between the latitudinal position of the monitoring sites and percentage of samples recorded under dry-deposition conditions.

3.2.1. Atmospheric deposition fluxes: soluble-inorganic particles

As seen in Fig. 3, the highest DF_{SOL} are recorded in the the natural area of Gallocanta (55,5 g m^{-2} $year^{-1}$), followed by the regional

Table 2
Insoluble, soluble and global annual atmospheric DF recorded in the DONAIRE network. Average June 2016–June 2017 but Frigiliana: September 2016–September 2017 and Gallocanta: August 2017–August 2018.

Site	Type of area	Insoluble	Soluble	Global
		g m^{-2} $year^{-1}$(% over global deposition)		
Cantabrian-Pyrenean region				
Enol	*Regional*	3,6 (10%)	30,9 (90%)	34,5
Orgi	*Regional*	3,5 (33%)	7,1 (67%)	10,6
Pamplona	*Urban*	6,8 (42%)	9,3 (58%)	16,1
Ordesa	*Regional*	16,3(53%)	14,3 (47%)	30,6
Ebro Valley region				
Chiprana	*Regional*	7,3 (50%)	7,4 (50%)	14,7
Almudévar	*Agricultural*	13,4 (48%)	13,3 (52%)	26,7
Gallocanta	*Regional*	10,0 (18%)	45,5 (82%)	55,5
Zaragoza	*Urban*	16,8 (54%)	14,2 (46%)	31,0
Monzón	*Industrial*	14,7 (50%)	14,5 (50%)	29,2
Ejea	Agricultural	20,7 (41%)	19,0 (59%)	39,7
Mediterranean region				
Montseny	*Regional*	6,3 (42%)	8,9 (58%)	15,2
Barcelona	*Urban*	9,6 (45%)	11,7 (55%)	21,3
H. Joan March	*Regional*	5,9 (30%)	13,6 (70%)	19,5
Palma	*Urban*	8,1 (28%)	20,6 (72%)	28,7
Frigiliana	*Regional*	13,7 (51%)	13,1 (49%)	26,8

background site of Enol (34,5 g m^{-2} $year^{-1}$), in the Picos de Europa National Park. On the other hand, the lowest DF_{SOL} are registered at the regional background site of Orgi, Chiprana and Montseny (7,1, 7,4 and 8,9 g m^{-2} $year^{-1}$, respectively), as well as at the urban sites of Pamplona and Barcelona (9,3 and 11,7 g m^{-2} $year^{-1}$, respectively). Intermediate concentrations (13,1–20,6 g m^{-2} $year^{-1}$) are observed at the other sites (Table 2). Moderate interannual variations are observed at sites having 2 or more years of data (see Section 3 in the Supplement), in most cases in connection with the amount of precipitation.

Fig. 4 depicts annual precipitation records and correlation coefficients (R) for each site, obtained from the comparison of DF_{SOL} against the accumulated precipitation for each sample. In general, R coefficients are above 0,5. The best correlations are observed in the Pyrenees and Almudévar (>0,80), followed by some coastal sites in the Mediterranean (0,69-0,76), and most of the Ebro Valley sites (0,59-0,66) as well as Barcelona, Frigiliana or Pamplona (0,42-0,57). On the contrary, the lowermost correlation is found in Enol, with no correlation found in Gallocanta. We can postulate that atmospheric deposition of soluble inorganic species is moderately-well connected to precipitation, which is suggesting that in most of the cases in-cloud scavenging processes are controlling the variability of such soluble-inorganic fluxes. Only in few cases DF_{SOL} are not varying in parallel with precipitation. The most extreme example is Gallocanta, where soil resuspension from salty lake sediments during dry periods inject huge amounts of soluble particles to the atmosphere.

In order to discern between the observed differences, Table 3 depicts the annual average DF_{SOL} separated.

in the main groups of compounds. The marine influence is registered especially in the Cantabrian site of Enol and in the two Balearic Islands sites, and its influence is clearly diminished towards inland areas in the Ebro Valley. However, two hotspots in the Ebro Valley are observed: Gallocanta and to a lesser extent, Ejea. The abundance of saline soils in the central Ebro Basin (Salvany et al., 2007), where Ejea is located, and the regular dryness of the Gallocanta lake (Comín et al., 1990; Luna Jordán, 2017), in combination with resuspension processes of different origin (agricultural activities over Ejea, wind resuspension over Gallocanta) may explain such above-normal values.

The **mineral dust** influence is surprisingly elevated in Enol, followed by Gallocanta and Ejea. Enol is the site registering the lowest impact of Saharan dust episodes and the site is surrounded by grass and shrublands, with little soil exposed to the open, which justifies discarding the impact of dust resuspension from local or regional origin. As a result, the most plausible explanation for such high values points to nearby anthropogenic sources, likely from the high concentration of coal-fired power plants in the surroundings and several metallurgical factories associated to the mining sector of the region. The official information from the Spanish Ministry of Energy records over 2100 MW of installed capacity in the Asturias region, where Enol is placed; around 2000 MW in the nearby Galicia region; and near 2000 MW of installed capacity in the adjacent Leon province. The use of carbonate rocks in the desulphurisation process could partially explain such high mineral matter concentrations. In addition, the metallurgic sector is not conceived without the use of lime, which is present throughout the entire transformation process. The addition of lime is required in electric arc furnaces and in converters, where it is used as a purifying agent, eliminating impurities, desulfurizing, dephosphorizing, acting as a flux or neutralizing. Therefore, most of the mineral dust observed at this site would be derived from the intense anthropogenic emissions occurring in the region. At other sites with lower (but still high in comparison) deposition of mineral dust, several different processes occur. That is the case of Gallocanta (wind-erosion of lagoon sediments), Ejea (agricultural dust), Monzón (industrial dusty emissions), Ordesa (highly impacted by African dust) or Zaragoza and Palma (probably affected by intense road dust emissions). Morales-Baquero et al., 2013 reported DF around 2,05 g m^{-2} $year^{-1}$ for the same components as included in this work in Sierra Nevada (SE Iberia), which are highly comparable to our observations in Frigiliana (2,56 g m^{-2} $year^{-1}$).

Non sea-salt sulfate aerosol DF was rather homogeneous and only much higher DF are observed over the Gallocanta region, surely due to the richness of Ca-sulfate species in local soils and in the lagoon

Fig. 3. Average DF_{SOL} (in g m^{-2} $year^{-1}$) registered in the DONAIRE network. Period: June 2016–June 2017 but Frigiliana: September 2016–September 2017 and Gallocanta: August 2017–August 2018.

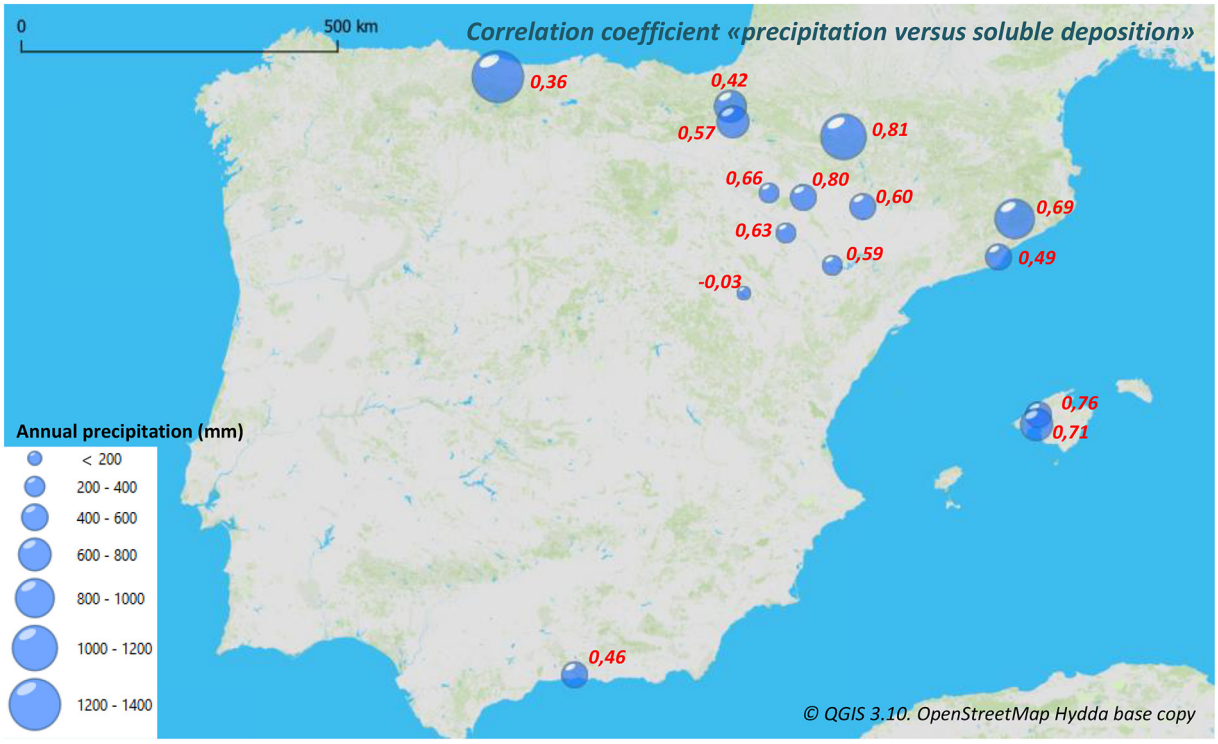

Fig. 4. Average annual precipitation (in mm) recorded at DONAIRE network sites. Values in red-colour indicate the correlation coefficient obtained between precipitation records and DF_{SOL}. Period: June 2016–June 2017, but Frigiliana: September 2016–September 2017 and Gallocanta: August 2017–August 2018.

(Comín et al., 1990; Luna Jordán, 2017), followed by Enol (probably connected to coal-fired and industrial emissions) and the Barcelona region (maybe reflecting the impact of industrial and shipping (Pey et al., 2013b)). In general, the overall sulphate DF fall in the typical ranges averaged in Im et al. (2013) and Vivanco et al. (2018) for our geographical domain. Avila et al., 2020 report sulphate DF for Montseny and two Pyrenean sites in Catalonia near the Val de Aran. When comparing our data with their observations, results at Montseny are fully comparable (1,4 g m^{-2} $year^{-1}$ against 1,3 g m^{-2} $year^{-1}$ in this study). However, our observations are lower than the Pyrenean ones (0,42 g m^{-2} $year^{-1}$ at Orgi and 0,93 g m^{-2} $year^{-1}$ at Ordesa, with respect to 1,0 g m^{-2} $year^{-1}$ and 1,5 g m^{-2} $year^{-1}$ at the two Val de Aran sites). The differences may be explained by spatial differences (our sites lying more to the west) or by a temporal mismatch (our recording was in 2016–2017, while the Val de Aran sites recorded between 1998 and 2014). Because sulphate deposition sharply decreased in this period (Avila et al., 2020), our results would need to be compared to the recent and lower deposition values in the Val de Aran record, not to the average which includes previous higher deposition. In the SE part of Iberia, Morales-Baquero et al., 2013 reported sulphate fluxes around 1,4 g m^{-2} $year^{-1}$ in Sierra Nevada (period 2001–2002), which contrast with the 0,78 g m^{-2} $year^{-1}$ measured in Frigiliana in this study. Again in this case, this would reflect the downward trens in sulphur deposition.

Table 3
Annual DF of the main clusters constituting the soluble-inorganic fraction Period: June 2016–June 2017, but Frigiliana: September 2016–September 2017 and Gallocanta: August 2017–August 2018. * Data from Ejea for the last part of the year (mid March-end June 2017 recovered by applying a proportional 1,33 factor).

g m^{-2} $year^{-1}$	Marine	Mineral	Nss SO_4^{2-}	N-species	PO_4^{3-}	HCO_3^-
Cantabrian-Pyrenean region						
Enol	7,21	6,05	1,00	2,02	2,30	12,87
Orgi	1,29	1,94	0,42	1,62	0,23	3,94
Pamplona	1,34	2,27	0,69	1,33	0,09	4,35
Ordesa	0,76	3,67	0,93	1,47	0,03	8,43
Ebro Valley region						
Chiprana	0,61	1,73	0,60	1,09	0,02	3,82
Almudévar	0,88	2,99	0,75	1,98	0,09	7,11
Gallocanta	4,02	5,66	2,38	10,78	1,05	18,28
Zaragoza	0,71	3,59	0,68	0,91	0,01	9,23
Monzón	0,83	3,68	0,64	1,50	0,09	8,07
Ejea*	2,45	3,99	0,88	0,88	0,06	10,89
Mediterranean region						
Montseny	2,19	1,93	1,29	1,57	0,01	3,01
Barcelona	2,88	2,61	1,07	1,58	0,01	4,75
Hospital Joan March	7,47	2,43	0,55	1,32	0,01	2,80
Palma	8,21	3,55	0,59	1,60	0,01	7,13
Frigiliana	2,83	2,56	0,78	1,71	0,03	5,20

The deposition of **nitrogen species** (NO_3^-, NO_2^- and NH_4^+) prevails in Gallocanta (10,78 g m^{-2} $year^{-1}$), and the concentration at other sites of the network are rather similar (0,88 to 2,02 g m^{-2} $year^{-1}$), reduced about one order of magnitude with respect to Gallocanta. The endorheic nature of the Gallocanta Basin, a declared Nitrate Vulnerable Zone, may act as a sink for nitrates to be accumulated in the lake (Comín et al., 1990). In the case of Frigiliana, our results (1,71 g m^{-2} $year^{-1}$) are comparable, but slightly lower, than those reported by Morales-Baquero for the Sierra Nevada in the SE Iberia (2,1–2,8 g m^{-2} $year^{-1}$, recorded in 2001–2002). Other available results for comparison are those reported by Avila et al. (2020) for Montseny (2,3 g m^{-2} $year^{-1}$), the Atlantic Pyrenees (2,5 g m^{-2} $year^{-1}$) and the Central Pyrenees (3,8 g m^{-2} $year^{-1}$), averaged for the period 2005–2014. In this study, they observed a progressive decrease in N-species deposion from 2006 onwards, thus, probably our current results fall in similar values as those measured at the end of their observations. The usual nitrogen-species DF fall in the range given by Vivanco et al. (2018) from an ensemble model intercomparison analysis for Europe.

DF of **phosphate** fall in the range of other studies at most sites of this network, as shown in the supplement, Section 3, where a comparative analysis with other studies in the Western Mediterranean is given.

However, phosphate deposition reached high values at various sites of the network, clearly above the typical ones reported in the literature (Bergametti et al., 1992; Guieu et al., 2002, 2010; Herut et al., 1999; Izquierdo, 2012; Markaki et al., 2010; Mahowald et al., 2008; or Morales-Baquero et al., 2006), in which typical annual fluxes bellow 0,02 g m^{-2} $year^{-1}$ for dissolved inorganic phospor are provided. This is the case of Enol (2,30 g m^{-2} $year^{-1}$), Gallocanta (1,05 g m^{-2} $year^{-1}$) and Orgi (0,23 g m^{-2} $year^{-1}$). In the first and third case, our hypothesis connects the emissions from coal-fired power plants and other industrial sources with the elevated concentrations observed, as high phospor levels are associated to certain combustion sources (Wang et al., 2015). In the second case, our postulate links the high phosphate and nitrate fluxes with agricultural dust, enriched in fertilizers. As seen in the supplementary file, such high values are not recorded constantly but they correspond to specific episodes. At Enol, most of phospapte peaks are well aligned with soluble Fe (results not shown in this article), K^+ and sulphate.

Finally, the amount of $\mathbf{HCO_3^-}$ is again enhanced in Gallocanta and Enol, and to a lesser extent in other sites in the Ebro Basin or in the Central Pyrenees. Fluxes of this compound varied in parallel with mineral ones (which are strongly driven by Ca^{2+}). Therefore, dissolution of carbonate particles governs the variability of dissolved inorganic carbon.

3.2.2. Atmospheric deposition fluxes: insoluble particles

DF_{INS} are depicted in Fig. 5. Most of regional background sites in northern Iberia recorded the lowest DF_{INS}, whereas the Ebro Valley area registered the highest ones. In general, DF_{INS} range from 3,5 g m^{-2} $year^{-1}$ in the regional background site of Orgi, in western side of the Pyrenees, to 16,3 and 16,8 g m^{-2} $year^{-1}$ in Ordesa and in the city of Zaragoza respectively, or 20,7 g m^{-2} $year^{-1}$ in the agricultural area of Ejea de los Caballeros. DF_{INS} over regional background sites ranged from 3,5 g m^{-2} $year^{-1}$ in Orgi to 16,3 g m^{-2} $year^{-1}$ in the Ordesa and Monte Perdido National Park, which is located only 100 km eastwards from the Orgi site. This sort of variability falls within the range presented by Vincent et al. (2016) for different sites in the Western Mediterranean. Our results from Frigiliana site (13,7 g m^{-2} $year^{-1}$) are comparable to those reported by Morales-Baquero for the Sierra Nevada mountain range, in the SE Iberia (10,9–11,3 g m^{-2} $year^{-1}$).

Important interannual variations can be observed at some sites having 2 or more years of data (see Section 3 in the Supplement), which in most cases are driven by the impact/absence of severe African dust deposition events. Section 4 in the supplement refers to periods with low and high DF and their seasonal variations. Herafter we discuss about DF_{INS} by investigating: 1) the regional resuspension in the Ebro Valley; 2) the influence of nearby atmospheric pollution sources, including urban-metropolitan and industrial emissions; 3) the climatic context; and 4) the impact of African dust.

3.3. Regional resuspension in the Ebro Valley

One of the pieces explaining the atmospheric phenomenology in our region refers to the emission of particles from the semi-arid Ebro Valley region. When regarding DF_{INS} at different regional background locations all over the network, after excluding the effect of African dust deposition (methodological details are given in Section 2.5), it becomes evident that the Ebro Valley region values are moderately higher (in the range 5,8–9,0 g m^{-2} $year^{-1}$, Ejea excluded) than those from the other two sub-regions: 2,8–3,8 g m^{-2} $year^{-1}$ in the Cantabrian and Pyrenean sector, and 3,3–4,6 g m^{-2} $year^{-1}$ in the Mediterranean area.

Considering the closest regional background sites to the so-called Ebro Valley subregion, namely Montseny and Ordesa, and considering $DF_{INS\text{-}NoAD}$ at these two sites (3,3 and 3,8 g m^{-2} $year^{-1}$, respectively; average contribution = 3,5 g m^{-2} $year^{-1}$) as the "pan-regional contribution", it is possible to estimate a range of insoluble deposition related to dust emisssions ($DF_{INS\text{-}REG}$) taking place in Ebro Valley (Table 4). In general, $DF_{INS\text{-}REG}$ ranges from 2,3 g m^{-2} $year^{-1}$ in Chiprana, 3,0 g m^{-2} $year^{-1}$ in the agricultural site of Almudévar, rising to 5,5 g m^{-2} $year^{-1}$ in Gallocanta and reaching 11,5 g m^{-2} $year^{-1}$ in the agricultural site of Ejea. Such regional contributions are strongly masked by local inputs in the last two sites. Overall, the relative contribution of regional dust to insoluble depositon fluxes in this region range between 22% to 30%, overpassing 50% in Gallocanta and Ejea owing to combined effect of regional and local emissions from arid soils.

3.4. Contribution of local sources: urban road dust

The influence of nearby pollution sources is a key factor to understand part of the observed phenomenology regarding insoluble aerosol fluxes. Since particulate matter pollution in urban and industrial areas is usually higher than in nearest regional background sites, the amount of deposited particles in such environments should be higher. Actually, urban and industrial areas registered higher DF_{INS} than their closest regional background sites (Fig. 5 and Table 2). In order to estimate the observed urban and industrial enhancement, Fig. 6 displays the urban and industrial contributions to DF_{INS} simultaneously at the urban (or industrial) sites together with those at their regional background. By appying the Lenschow et al. (2001) approach (urban or industrial minus regional background, e.g., Pamplona-Orgi, Zaragoza-Chiprana, Barcelona-Montseny, Palma-H. Joan March, and Monzón-Chiprana), the estimation of urban and industrial contributions to insoluble deposition are calculated. Given that the impact of AD is relevant and it may differ considerably in short distances, we have used $DF_{INS\text{-}NoAD}$ values to estimate annual fluxes. In general, annual DF_{INS} from urban-metropolitan origin ($DF_{INS\text{-}URB}$) ranged between 2,6 and 3,9 g m^{-2} $year^{-1}$ (37–41% of the recorded DF_{INS} in these cities). The city of Zaragoza registered much higher $DF_{INS\text{-}URB}$ amounts (7,5 g m^{-2} $year^{-1}$, 45% of DF_{INS}), as it is located in the Ebro Valley, in which $DF_{INS\text{-}REG}$ occurs (from 2,3 to 3,0 g m^{-2} $year^{-1}$, see previous section) and higher frequency dry periods (see Fig. 2) take place, both factors keeping urban streets dustier than in the other three cities.

Regarding the industrial city of Monzón (17.000 inhabitants), $DF_{INS\text{-}URB}$ were comparable to those observed in Zaragoza (675.000 inhabitants), 8,0 g m^{-2} $year^{-1}$ (Fig. 6), but in this case with a clear impact from industrial emissions occurring next to the monitoring site: an old foundry with two silicomanganese and two ferromanganese furnaces, a calcium carbide production factory, a chemical plant focused on chloride production, and a factory in which sand, gravels and other materials for concrete production are processed. Overall, $DF_{INS\text{-}URB}$ at Monzón accounted for around 55% of the recorded insoluble deposition in Monzón.

3.5. Deposition fluxes of insoluble particles in a climatic context

When regarding annual DF_{INS} against precipitation, and grouping the sites according to their geographical position, a number of details can be observed (Fig. 7A). In general, 14 out of 15 sites follow perfectly one of the two trend lines. One of these lines only contains a number of regional background sites and could include or not the city of Pamplona (R^2 = 0,78); and the other line, starts in the cleanest regional background site from the Cantabrian-Pyrenean region, Orgi, and ends in the dustiest area in the Ebro Valley, Ejea, passing through all urban sites, the agricultural ones, the industrial site of Monzón and the southernmost regional background site, Frigiliana (R^2 = 0,75). Only Ordesa is excluded of these lines, as it was two times impacted by severe Saharan dust depostion events. In order to avoid the interference of African dust in this analysis, the same Figure has been elaborated removing from the database those samples impacted by Saharan dust (Fig. 7B). The most interesting feature is that all regional background sites follow a well defined potential curve (R^2 = 0,73), while the rest of the observatories are aligned in a very different distribution (R^2 = 0,89), taking out from the line the industrial site of Monzón, otherwise the R^2 coefficient decrease to 0,59.

Fig. 5. Average insoluble atmospheric DF (g m^{-2} $year^{-1}$) registered in the DONAIRE network. Period: June 2016–June 2017, but Frigiliana: September 2016–September 2017 and Gallocanta: August 2017–August 2018.

From this analysis the prediction of DF_{INS} at other regional or urban areas in the studied region could be possible, as they vary in parallel with aridity. Such increment is very pronounced at sites where anthropogenic emissions take place. In our case, the impact of regional, agricultural, urban and industrial dust is enhanced as far as the precipitation decreases.

3.6. Impact of African dust

Certain sites of the network registered a much higher impact of African dust than others located in the same region or at short distances. Although a downward trend in African dust frequency occurs from southern sites to northern ones (from around 30% of the annual days to <10% in the North or 15% in the NE of Iberia, according to Pey et al., 2013a), the findings regarding dust-deposition does not follow that gradation. Table 5 shows average $DF_{SOL\text{-}NoAD}$ and $DF_{INS\text{-}NoAD}$, and the estimate of African dust contributions $DF_{INS\text{-}AD}$ and $DF_{SOL\text{-}AD}$ by applying the two approaches described in Section 2.5.

As seen in Table 5, the site registering the highest $DF_{INS\text{-}AD}$ and $DF_{SOL\text{-}AD}$ was Ordesa (Central Pyrenees), followed by Frigiliana (SE of Iberia), and Almudévar and Ejea (in the northern side of the Ebro Valley, close to the Pre-Pyrenees geographical barrier). It is interesting to remark that nearby areas like Orgi (in the Atlantic Pyrenees) are registering negligible desert dust concentrations when compared to Ordesa (Table 5). Our hypothesis is that the Pyrenees are acting as a natural barrier for dusty air masses travelling northwards, creating a prominent Föehn effect during certain meteorological situations. This fact may cause an enhancement of African dust deposition with altitude, an effect that may be diluted as altitude decreases. To illustrate this phenomenon, Fig. 8 depicts a northern-southern transect from Ordesa to Frigiliana passing through Almudévar and Chiprana, of one of the two severe dust episodes recorded during the period under study. During this event, Ordesa recorded the most important dust flux, followed by Frigiliana. A progressive downward trend in dust deposition occurred as far as the distance to the Pyrenees increased. These patterns are strogly related to wet-deposion of African dust (or red rains), as detailed in the supplement (Section S4).

Our method also suggests an important $DF_{SOL\text{-}AD}$ contribution. Actually, Fu et al., 2017 have demonstrated that important dissolution of certain components take place in this region of the Mediterranean on weekly samples, which could be accentuated in the case of our 15-monitoring intervals. See Section 4.2 in the supplement for further details. Note that $DF_{SOL\text{-}noAD}$ increases in parallel with precipitation in most cases (Fig. 4), and therefore the estimation of $DF_{SOL\text{-}AD}$ could be partially biased.

Table 4
DF_{INS} (in g m^{-2} $year^{-1}$) recorded in the DONAIRE network, average fluxes recalculated after subtracting African dust $DF_{INS\text{-}NoAD}$. Estimation of Regional ($DF_{INS\text{-}REG}$) contribution ranges by difference, considering the registers from Montseny and Ordesa (in bold).

g m^{-2} $year^{-1}$	Type area	DF_{INS}	$DF_{INS\text{-}NoAD}$	$DF_{INS\text{-}REG}$
Cantabrian-Pyrenean region				
Enol	Regional	3,6	3	
Orgi	Regional	3,5	2,8	
Ordesa	Regional	16,3	**3,8**	
Ebro Valley region				
Chiprana	Regional	7,3	5,8	**2,3**
Gallocanta	Regional	10	9	**5,5**
Almudévar	Agricultural	13,4	6,5	**3,0**
Ejea[a]	Agricultural	20,7	15	**11,5**
Mediterranean region				
Montseny	Regional	6,3	**3,3**	
Joan March	Regional	5,9	4,6	
Frigiliana	Regional	13,7	4,3	

[a] Agricultural area in which local emissions do not represent the atmospheric phenomenology of the entire region.

4. Discussion and conclusions

In the context of the DONAIRE project, a network of 15 atmospheric-deposition monitoring sites was built in Spain, covering latitudinal,

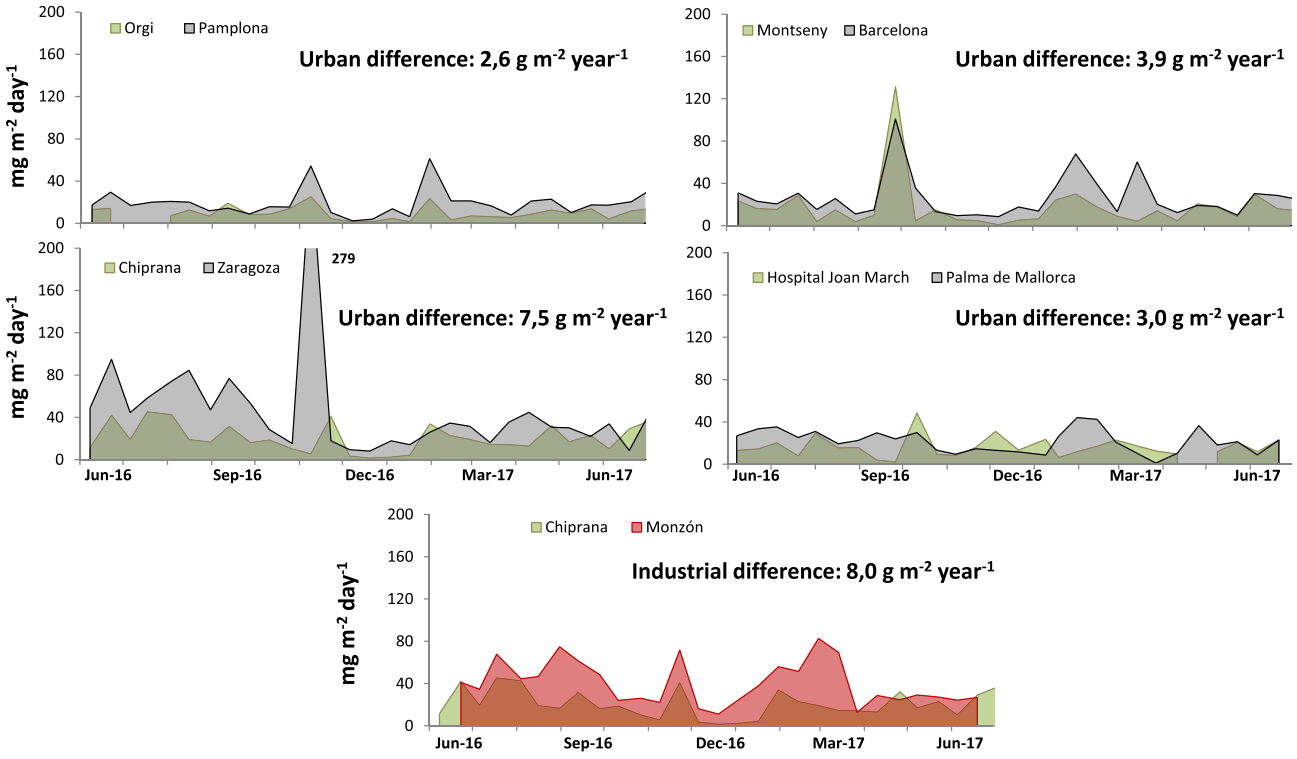

Fig. 6. DF_{INS} registered at urban/industrial sites, together with those at their reference regional background areas (in mg m^{-2} day^{-1}) during the studied period (June 2016–June 2017). Estimation of annual urban or industrial contributions following the Lenschow et al. (2001) approach.

longitudinal and altitudinal gradients, different degrees of anthropogenic influence, and various climatic contexts. This network has evidenced that atmospheric deposition varies considerably across the studied region, ranging from annual fluxes around 10 g m^{-2} in the "cleanest" areas to around 40 g m^{-2} in the "dustiest" ones, with even higher values near hotspots of dust mobilization. When analyzing the partitioning between DF_{SOL} and DF_{INS} we observe a reasonable gradation of DF_{SOL} from coastal regions towards inland sites. This was especially obvious in Enol where, after Gallocanta, the highest DF_{SOL} records occurred, in part because of the arrival of marine aerosols from the Cantabrian Sea, but especially because of the contribution of anthropogenic emissions (N-species, S-species, phosphates, and mineral particles) from a variety of anthropogenic emissions occurring in nearby areas. Actually, the amount of phosphate deposited in this area exceeds the typical values observed in Western Europe. In the two highest cases, our values are considerably higher than those observed near fugitive phosphogypsum emissions in SW Iberia (Torres-Sánchez et al., 2019), which measured annual fluxes around 0,8 g m^{-2} $year^{-1}$ and rapidly decreasing to 0,2 g m^{-2} $year^{-1}$ at only 1,5 km to source areas. Our observations need to be further confirmed by monitoring in

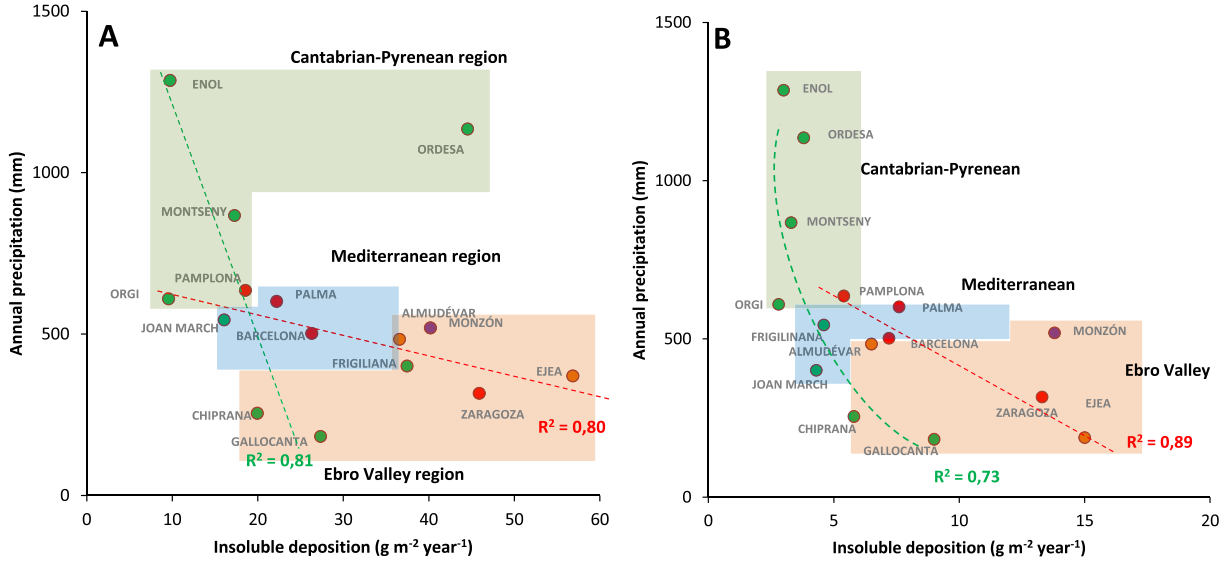

Fig. 7. Relationship between annual precipitation (in mm) and insoluble deposition (in g m^{-2} $year^{-1}$) at all sites in the DONAIRE network. A: all data; B: all data excluding African dust.

Table 5
$DF_{INS\text{-}NoAD}$ and $DF_{SOL\text{-}NoAD}$ recorded in the DONAIRE network. Estimation of AD fluxes ($DF_{INS\text{-}AD}$ and $DF_{SOL\text{-}AD}$) by applying the two methods (M1 and M2) described in Section 2.5.

Site	Type area	$DF_{INS\text{-}NoAD}$	$DF_{SOL\text{-}NoAD}$	$DF_{INS\text{-}AD}$	$DF_{INS\text{-}AD}$	$DF_{SOL\text{-}AD}$	$DF_{SOL\text{-}AD}$
$g\ m^{-2}\ year^{-1}$				M1	M2	M1	M2
Cantabrian-Pyrenean region							
Enol	Regional	3	32	0,5	0,5	0	0
Orgi	Regional	2,8	6,1	0,7	0,7	0,9	0,9
Pamplona	Urban	5,4	8,1	1,3	1,5	1,2	1,8
Ordesa	Regional	3,8	5,1	12,4	13,2	9,3	9,7
Ebro Valley region							
Chiprana	Regional	5,8	6,6	1,5	1,7	0,7	0,9
Almudévar	Agricultural	6,5	8,6	6,9	7,4	4,7	5,1
Gallocanta	Regional	9	45,9	1	0	0	0
Zaragoza	Urban	13,3	11,8	3,4	4,3	2,4	2,7
Monzón	Industrial	13,8	13,5	0,9	1,2	1	1,4
Ejea	Agricultural	15	14,3	5,7	4,7	4,7	3,8
Mediterranean region							
Montseny	Regional	3,3	8,4	3	2,8	0,5	1,2
Barcelona	Urban	7,2	12,1	2,4	2,3	0	0,8
H. Joan March	Regional	4,6	11,7	1,2	1,7	1,9	3,8
Palma	Urban	7,6	22,2	0,5	1	0	1,1
Frigiliana	Regional	4,3	7,5	9,4	9,4	5,6	5,6

nearby areas and/or by collecting parallel samples with other devices but, in case our values are corroborated, the ecological equilibrium of the iconic Lake Enol could be in risk. This ecosystem already suffers hypolimnetic anoxia for other reasons (Sánchez-España et al., 2017). In the Mediterranean coast of the Iberian Peninsula and the Balearic Islands, DF_{SOL} is moderately enhanced when compared to inland locations, and in those cases the role of marine aerosols is crucial to explain such divergences. However, the second hotspot of DF_{SOL} is found in the Natural Reserve of Gallocanta (the furthest site to the coast), a saline endorheic lake system periodically dried. During the studied period, the lake was totally or partially desiccated during several months and, under these conditions, the occurrence of intense winds from the northwest favored the resuspension of lake sediments, causing an intense remobilization of salts and dust particles at the regional scale, as discussed in Comín et al. (1990).

DF_{INS} represents around 10% to 50% of the global fluxes. Such DF are especially enhanced in the Ebro Valley, which is a vast semi-arid region occupying 7% of the Iberian Peninsula, followed by the Central Pyrenees and the southernmost part of this network. The emission of dust particles from Ebro Basin soils play a significant role in these observations. Actually, we have estimated that $DF_{INS\text{-}REG}$ accounts for 20–34% of DF_{INS} at this region. These results underline the importance of regional

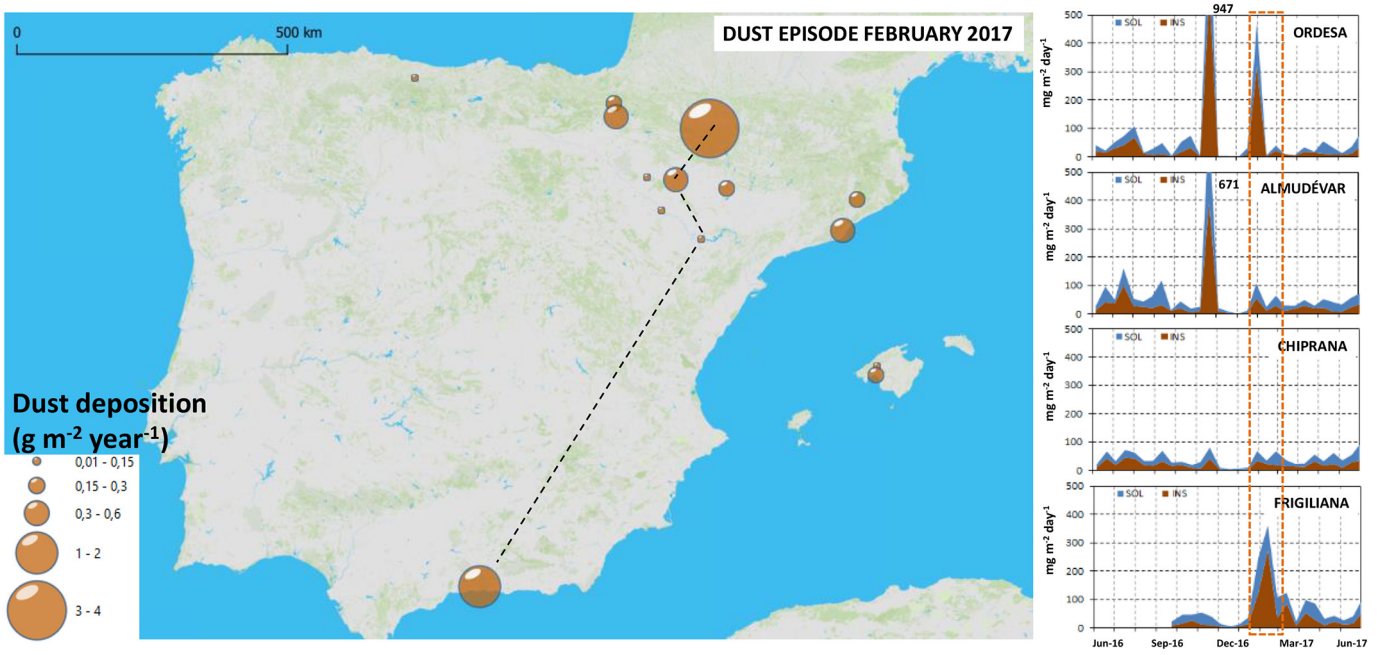

Fig. 8. Left: map showing the annual contribution to DF_{INS} (in g m^{-2} $year^{-1}$) registered in the DONAIRE network as a result of the February 2017 dust event. Right: northern-southern transect illustrating DF_{SOL} and DF_{INS} (in mg m^{-2} day^{-1}) recorded at these four sites, illustrating the severity of the February 2017 event in Ordesa and Frigiliana. Note also the impact of the November 2016 episodes in Ordesa and Almudévar.

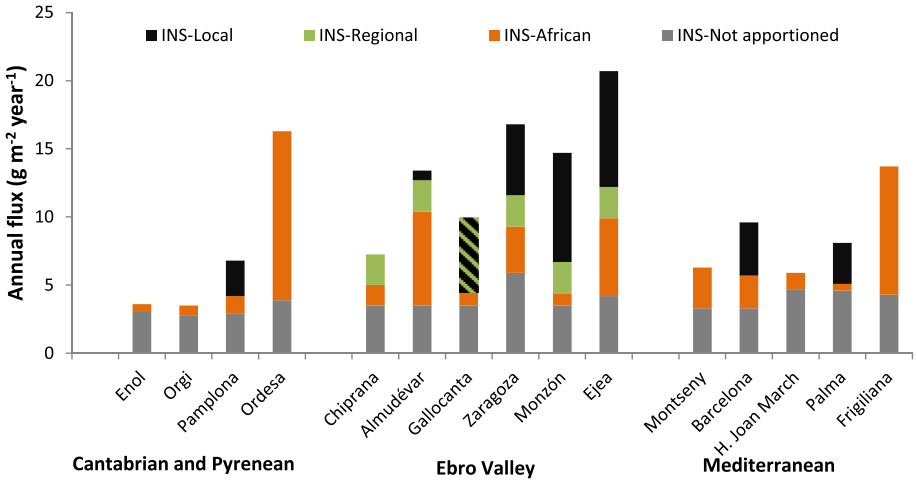

Fig. 9. Partitioning of insoluble (INS) atmospheric DF (local, regional, African and not-apportioned) at the 15 sites of the DONAIRE network.

dust resuspension in this vast territory in which >3 million inhabitants are living. Our results show that regional dust emissions are an important source of aerosols, a contribution that up to now has not been quantified. Further work should address the role of these regional emission on $PM_{2.5}$ and PM_{10} concentrations in the Ebro valley in order to better understand the phenomenology of dust emission in this region, and to what extent this phenomenon could exceed the limits of the Ebro Basin.

Two other hotspots of DF_{INS} in the edges of the network are observed. In both cases the deposition of African dust explains such high values and, due to its episodic nature, important inter-annual variations may occur (Avila et al., 2020) as it happened in the period 2016–2019. Similar deposition was observed in the southernmost site of Frigiliana and the central Pyrenees (9 vs 12–13 g m^{-2} $year^{-1}$), despite the fact that the number of African dust outbreaks was triple in the south site (30–35 vs 10–15%). Our monitoring strategy has lead us to infer the occurrence of a Föehn effect that would explain an enhanced scavenging of African dust in the Pyrenees. In parallel, these observations have released some other questions: *What is happening in other mountain barriers located southwards, such as the Iberian or the Penibetic Ranges?* or *How much the Pyrenees are "cleaning" the air masses travelling northwards during these situations?,* or *What would be observed if a northern-southern transect in the same region of the Pyrenees is done?*. Besides these questions, there is an intrinsic interest in studying the deposition of African dust particles since they are enriched in certain nutrients (Àvila and Rodà, 1991; Àvila and Peñuelas, 1999) or they carry a wide variety of microorganisms (Cáliz et al., 2018). Thus, the identification of "African-dust-deposition hotspots" may be helpful when, in natural areas, management/protection measures on certain ecosystems are implemented.

At urban areas and at Monzón 37–45% and 55% of DF_{INS}, respectively, is related to local contributions. Most likely, road dust resuspension and industrial exhauts, respectively, are behind those contributions, although the input from other urban-to-metropolitan sources could not be disregarded. Thus, the city of Pamplona, which is the one in between Atlantic and Mediterraean climates, registered a comparable amount of local to metropolitan contributions to Palma. Bearing in mind that Pamplona lists around 100 days/year of rain >1 mm, while Zaragoza, Barcelona and Palma record only 50–60 days/year, and considering the results by Amato et al. (2012), in which they demonstrated that urban road dust is promptly recovered after rain events, the local contribution associated to urban road dust should be less significant in Pamplona if urban road dust would be the main source at such local inputs. Accordingly, the impact of other metropolitan emissions at this site is potentially playing a role. The investigation of the chemical composition of insoluble particles and the identification of the sources will put light on these outcomes. The situation in the case of Zaragoza is rather different: $DF_{INS\text{-}URB}$ is highly accentuated with respect to the other cities. The enhanced dust supplied by the dust emissions at the regional scale and the high number of dry periods could result in much higher road dust loads in urban streets, as observed by Amato et al. (2014) in different Andalusian cities (also in dry climates) when compared their values to the usual ranges. A significant part of DF_{INS} near agricultural and industrial sites is related to local contributions, as evidenced in Ejea and Monzón, respectively.

Fig. 9 condenses all the estimates retrieved from the study regarding DF_{INS}. As seen in Fig. 9, the "not-apportioned" part of the insoluble DF, which could be considered as the continental input at this region, ranges in a narrow interval, from 3 to 6 g m^{-2} $year^{-1}$.

The results of the DONAIRE network provide new insights regarding pan-regional aerosol deposition in contrasted environments in south-western Europe. The main limitation of our monitoring devices is the integration of dry and wet deposition, which is limiting our full-understanding of the atmospheric phenomenology in the studied area.

Declaration of competing interest

The authors declare that they have no known competing financial interests or personal relationships that could have appeared to influence the work reported in this paper.

Acknowledgements

This work has been possible thanks to financial support from the Spanish Agencia Estatal de Investigación and the European Funds for Regional Development (AEI/FEDER, UE) via the DONAIRE (CGL2015-68993-R) project.

We would like to thank Pedro Zuazo and Javier Vera, from the Regional Government of Navarra; Guillermo Sánchez and Pilar Pérez Colomina, from the Regional Government of Aragón; Paula Elías, from the Regional Government of the Balearic Islands; Nieves Fernández, from the Ayuntamiento de Zaragoza; Alejandro Herrero y Antonio Manuel López, from the Ayuntamiento de Frigiliana; Amparo Mora, from the Picos de Europa National Park; Elena Villagrasa, from the Ordesa and Monte Perdido National Park; Javier Gómez and Edurne Gerendiain, from Garrapo S.L.; and Cristina Salas, from VIESGO S.L. for their administrative support and the consent to access the facilities used in this project. A special thank is given to the group of technicians giving support in this project: Ángel Tejedor, from the Picos de Europa National Park; Fran Bayo, from Aguirre S.L.; and the personnel of the Ordesa y Monte Perdido National Park.

The authors gratefully acknowledge the BSC dust deposition products (http://www.bsc.es/projects/earthscience/visor/dust/med8/dep/archive/), the NOAA Air Resources Laboratory (ARL) for the provision of the HYSPLIT transport and dispersion model and/or READY website (http://www.ready.noaa.gov) used to interpret some data of this publication, and the Spanish Meteorological Agency (AEMET, www.aemet.es) for the provision of meteorological data from different observatories.

Maps generated for this article have been produced thanks to the QGIS (http://qgis.osgeo.org) Development Team (2018), v 3.10, by using the OpenStreetMap Hydda base copy.

Finally, we would like to thank the three reviewers of this manuscript for their helpful suggestions.

Author contributions

Jorge Pey and Juan Cruz Larrasoaña designed the study and performed the data analysis. Jorge Pey wrote the article, receiving inputs from the rest of the co-authors in different sections of the article. Juan Cruz Larrasoaña (Navarra), Jorge Pey and Tania Mochales (Aragón), Noemí Pérez (Catalonia), José Carlos Cerro and Maria Luisa Tobar (Balearic Islands), Mª Pilar Mata (Picos de Europa), José María Orellana and Jesús Causapé (Gallocanta area) and Sonia Castillo (Frigiliana) were responsible of the coordination and monitoring in their respective areas. Jesús Reyes, Amalia de Vergara and Icíar Vázquez were the responsible of laboratory data management and analytical determinations. All the coauthors contributed to the final version of this article.

Data availability

Data from the repository can be used in other studies by including the authorship of the DONAIRE team: Jorge Pey[1], Juan Cruz Larrasoaña[2], Noemí Pérez[3], José Carlos Cerro[4,5], Sonia Castillo[6,7], María Luisa Tobar[4], Amalia de Vergara[8], Icíar Vázquez[8], Jesús Reyes[8], María Pilar Mata[8], Tania Mochales[2], José María Orellana[2], Jesús Causapé[2].

[1] ARAID – Instituto Pirenaico de Ecología (CSIC). 50,059 Zaragoza, Spain.

[2] Instituto Geológico y Minero de España. 50,006 Zaragoza, Spain.

[3] Instituto de Diagnóstico Ambiental y Estudios del Agua (CSIC). C/ Jordi Girona 18–26, 08028 Barcelona, Spain.

[4] Laboratory of the Atmosphere, Govern Illes Balears. 07009 Palma de Mallorca, Spain.

[5] Laboratory of Environmental Analytical Chemistry, Illes Balears University. 07122 Palma de Mallorca, Spain.

[6] Andalusian Institute for Earth System Research (IISTA-CEAMA). 18,071 Granada, Spain.

[7] Department Applied Physics, University of Granada. 18,071 Granada, Spain.

[8] Instituto Geológico y Minero de España. 28,760 Tres Cantos, Spain.

Appendix A. Supplementary data

Supplementary data associated with this article can be found in the online version, at https://doi.org/10.1016/j.scitotenv.2020.140745. These data include the Google map of the most important areas described in this article.

References

Alastuey, A., Querol, X., Chaves, A., Ruiz, C.R., Carratalá, A., López Soler, A., 1999. Bulk deposition in a rural area located around a large coal-fired power station, Northeast Spain. Environ. Pollut. 106, 359–367. https://doi.org/10.1016/S0269-7491(99)00103-7.

Amato, F., Schaap, M., Denier van der Gon, H.A.C., Pandolfi, M., Alastuey, A., Keuken, M., Querol, X., 2012. Effect of rain events on the mobility of road dust load in two Dutch and Spanish roads. Atmos. Environ. 62, 352–358. https://doi.org/10.1016/j.atmosenv.2012.08.042.

Amato, F., Alastuey, A., de la Rosa, J., Gonzalez Castanedo, Y., Sánchez de la Campa, A.M., Pandolfi, M., Lozano, A., Contreras González, J., Querol, X., 2014. Trends of road dust emissions contributions on ambient air particulate levels at rural, urban and industrial sites in southern Spain. Atmos. Chem. Phys. 14, 3533–3544. https://doi.org/10.5194/acp-14-3533-2014.

Appleby, P.G., Koulikov, A.O., Camarero, L., Ventura, M., 2002. The input and transmission of fallout radionuclides through Redó, a high mountain lake in the Spanish Pyrenees. Water Air Soil Poll. 2, 19–31. https://doi.org/10.1023/A:1020129919765.

Àvila, A., 1996. Time trends in the precipitation chemistry at a mountain site in northeastern Spain for the period 1983-1994. Atmos. Environ. 30, 1363–1373.

Àvila, A., Peñuelas, J., 1999. Increasing frequency of Saharan rains over northeastern Spain and its ecological consequences. Sci. Total Environ. 228, 153–156. https://doi.org/10.1016/S0048-9697(99)00041-8.

Àvila, A., Rodà, F., 1991. Red rains as major contributors of nutrients and alkalinity to terrestrial ecosystems at Montseny (NE Spain). Orsis 6, 215–229.

Àvila, A., Rodà, F., 2012. Changes in atmospheric deposition and stream water chemistry over 25 years in undisturbed catchments in a Mediterranean mountain environment. Sci. Total Environ. 434, 18–27. https://doi.org/10.1016/j.scitotenv.2011.11.062.

Àvila, A., Molowny-Horas, R., Gimeno, B.S., Peñuelas, J., 2010. Analysis of decadal time series in wet N concentrations at five rural sites in NE Spain. Water Air Soil Poll. 207, 123–138. https://doi.org/10.1007/s11270-009-0124-7.

Avila, A., Molowny-Horas, R., Camarero, L., 2020. Stream chemistry response to changing nitrogen and sulfur deposition in two mountain areas in the Iberian Peninsula. Sci. Total Environ. 711, 134697.

Bacardit, M., Camarero, L., 2009. Fluxes of Al, Fe, Ti, Mn, Pb, Cd, Zn, Ni, Cu and As in monthly bulk deposition over the Pyrenees (SW Europe): the influence of meteorology on the atmospheric component of the trace element cycles and its implications for high mountain lakes. J. Geophys. Res-Biogeo. 114, G00D02. https://doi.org/10.1029/2008JG000732.

Bacardit, M., Camarero, L., 2010a. Major and trace elements in soils in the Central Pyrenees: high altitude soils as a cumulative record of background atmospheric contamination over SW Europe. Environ. Sci. Pollut. R. 9, 1606–1621. https://doi.org/10.1007/s11356-010-0349-4.

Bacardit, M., Camarero, L., 2010b. Atmospherically deposited major and trace elements in the winter snowpack along a gradient of altitude in the Central Pyrenees: the seasonal record of long-range fluxes over SW Europe. Atmos. Environ. 44, 582–595. https://doi.org/10.1016/j.atmosenv.2009.06.022.

Bergametti, G., Remoudaki, E., Losno, R., Steiner, E., Chatenet, B., Buat-Ménard, P., 1992. Source, transport and deposition of atmospheric phosphorus over the northwestern Mediterranean. J. Atmos. Chem. 14, 501–513.

Bobbink, R., Hicks, K., Galloway, J., Spranger, T., Alkemade, R., Ashmore, M., Bustamante, M., Cinderby, S., Davidson, E., Dentener, F., Emmett, B., Erisman, J.-W., Fenn, M., Gilliam, F., Nordin, A., Pardo, L., De Vries, W., 2010. Global assessment of nitrogen deposition effects on terrestrial plant diversity: a synthesis. Ecol. Appl. 20, 30–59. https://doi.org/10.1890/08-1140.1.

Cáliz, J., Triadó-Margarit, X., Camarero, L., Casamayor, E.O., 2018. A long-term survey unveils strong seasonal patterns in the airborne microbiome coupled to general and regional atmospheric circulations. P. Natl. Acad. Sci. 115, 12229–12234. https://doi.org/10.1073/pnas.1812826115.

Camarero, L., Botev, I., Muri, G., Psenner, R., Rose, N., Stuchlik, E., 2009. Trace elements in alpine and arctic lake sediments as a record of diffuse atmospheric contamination across Europe. Freshw. Biol. 54, 2518–2532. https://doi.org/10.1111/j.1365-2427.2009.02303.x.

Castillo, S., de la Rosa, J.D., Sánchez de la Campa, A.M., González-Castanedo, Y., Fernández-Camacho, R., 2013a. Heavy metal DF affecting an Atlantic coastal area in the southwest of Spain. Atmos. Environ. 77, 509–517. https://doi.org/10.1016/j.atmosenv.2013.05.046.

Castillo, S., de la Rosa, J., Sánchez de la Campa, A., González-Castanedo, Y., Fernández-Caliani, J.C., González, I., Romero, A., 2013b. Contribution of mine wastes to atmospheric metal deposition in the surrounding area of an abandoned heavily polluted mining district (Rio Tinto mines, Spain). Sci. Total Environ. 449, 363–372. https://doi.org/10.1016/j.scitotenv.2013.01.076.

Castillo, S., Alastuey, A., Cuevas, E., Querol, X., Ávila, A., 2017. Quantifying dry and wet DF in two regions of contrasted African influence: the NE Iberian Peninsula and the Canary Islands. Atmosphere 8, 86. https://doi.org/10.3390/atmos8050086.

Comín, F.A., Julià, R., Comín, M.P., Plana, F., 1990. Hydrogeochemistry of Lake Gallocanta. (Aragón, NE Spain). Hydrobiologia 197, 51–66.

EEA, 2013. Air quality in Europe — 2013 report. European Environment Agency Technical Report No. 9/2013 Available on-line at. http://www.eea.europa.eu.

Fernández-Olmo, I., Puente, M., Irabien, A., 2015. A comparative study between the fluxes of trace elements in bulk atmospheric deposition at industrial, urban, traffic, and rural sites. Environ. Sci. Pollut. Res. 22, 13427–13441.

Fu, Y., Desboeufs, K., Vincent, J., Bon Nguyen, E., Laurent, B., Losno, R., Dulac, F., 2017. Estimating chemical composition of atmospheric deposition fluxes from mineral insoluble particles deposition collected in the western Mediterranean region. Atmos. Meas. Tech. 10, 4389–4401. https://doi.org/10.5194/amt-10-4389-2017.

Galloway, J.N., Townsend, A.R., Erisman, J.W., Bekunda, M., Cai, Z.C., Freney, J.R., Martinelli, L.A., Seitzinger, S.P., Sutton, M.A., 2008. Transformation of the nitrogen cycle: recent trends, questions, and potential solutions. Science 320, 889–892. https://doi.org/10.1126/science.1136674.

García-Gómez, H., Garrido, J.L., Vivanco, M.G., Lassaletta, L., Rábago, I., Àvila, A., Tsyro, S., Sánchez, G., González Ortiz, A., González-Fernández, I., Alonso, R., 2014. Nitrogen deposition in Spain: modeled patterns and threatened habitats within the Natura 2000 network. Sci. Total Environ. 485-486, 450–460. https://doi.org/10.1016/j.scitotenv.2014.03.112.

Guieu, C., Löye-Pilot, M.D., Ridame, C., Thomas, C., 2002. Chemical characterization of the Saharan dust end-member: some biogeochemical implications for the western Mediterranean Sea. J. Geophys. Res. 107 (D15), 4258.

Guieu, C., Löye-Pilot, M.D., Benyahya, L., Dufour, A., 2010. Spatial variability of atmospheric fluxes of metals (Al, Fe, Cd, Zn and Pb) and phosphorus over the whole Mediterranean from a one-year monitoring experiment: biogeochemical implications. Mar. Chem. 120, 164–178.

Herut, B., Krom, M.D., Pan, G., Mortimer, R., 1999. Atmospheric input of nitrogen and phosphorus to the Southeast Mediterranean: sources, fluxes, and possible impact. Limnol. Oceanogr. 44, 1683–1692.

Hou, P., Wu, S., McCarty, J.L., Gao, Y., 2018. Sensitivity of atmospheric aerosol scavenging to precipitation intensity and frequency in the context of global climate change. Atmos. Chem. Phys. 18, 8173–8182. https://doi.org/10.5194/acp-18-8173-2018.

Im, U., Christodoulaki, S., Violaki, K., Zarmpas, P., Kocak, M., Daskalakis, N., Mihalopoulos, N., Kanakidou, M., 2013. Atmospheric deposition of nitrogen and sulfur over southern Europe with focus on the Mediterranean and the Black Sea. Atmos. Environ. 81, 660–670. https://doi.org/10.1016/j.atmosenv.2013.09.048.

Izquierdo, R., 2012. Source Areas and Atmospheric Transport Processes of Chemical Compounds and Pollen in the NE Iberian Peninsula and the Canary Islands. Universitat Autònoma de Barcelona PhD Thesis.

Izquierdo, R., Àvila, A., 2012. Comparison of collection methods to determine atmospheric deposition in a rural Mediterranean site (NE Spain). J. Atmos. Chem. 69 (4), 351–368.

Izquierdo, R., Benítez-Nelson, C.R., Masqué, P., Castillo, S., Alastuey, A., Ávila, A., 2012. Atmospheric phosphorus deposition in a near-coastal rural site in the NE Iberian Peninsula and its role in marine productivity. Atmos. Environ. 49, 361–370. https://doi.org/10.1016/j.atmosenv.2011.11.007.

Izquierdo, R., Alarcón, M., Aguillaume, L., Ávila, A., 2014. Effects of teleconnection patterns on the atmospheric routes, precipitation and deposition amounts in the North-Eastern Iberian Peninsula. Atmos. Environ. 89, 482–490. https://doi.org/10.1016/j.atmosenv.2014.02.057.

Jordi, A., Basterretxea, G., Tovar Sánchez, A., Alastuey, A., Querol, X., 2012. Copper aerosols inhibit phytoplankton growth in the Mediterranean Sea. P. Natl. Acad. Sci. 109, 21246–21249. https://doi.org/10.1073/pnas.1207567110.

Lenes, J.M., Darrow, B.P., Cattrall, C., Heil, C.A., Callahan, M., Vargo, G.A., Byrne, R.H., Prospero, J.M., Bates, D.E., Fanning, K.A., Walsh, J.J., 2001. Iron fertilization and the Trichodesmium response on the West Florida shelf. Limnol. Oceanogr. 46, 1261–1277. https://doi.org/10.4319/lo.2001.46.6.1261.

Lenschow, P., Abraham, H.J., Kutzner, K., Lutz, M., Preuβ, J.D., Reichenbächer, W., 2001. Some ideas about the sources of PM10. Atmos. Environ. 35, S23–S33. https://doi.org/10.1016/S1352-2310(01)00122-4.

Luna Jordán, E., 2017. Suelos de un humedal salino y fluctuante: la Laguna de Gallocanta. University of Zaragoza PhD Thesis (in Spanish).

Mahowald, N., Jickells, T.D., Baker, A.R., Artaxo, P., Benitez-Nelson, C.R., Bergametti, G., Bond, T.C., Chen, Y., Cohen, D.D., Herut, B., Kubilay, N., Losno, R., Luo, C., Maenhaut, W., McGee, K.A., Okin, G.S., Siefert, R.L., Tsukuda, S., 2008. Global distribution of atmospheric phosphorus sources, concentrations and deposition rates, and anthropogenic impacts. Global Biogeochem. Cy. 22, GB4026. https://doi.org/10.1029/2008GB003240.

Mahowald, N.M., Engelstaedter, S., Luo, C., Sealy, A., Artaxo, P., Benitez-Nelson, C., Bonnet, S., Chen, Y., Chuang, P.Y., Cohen, D.D., Dulac, F., Herut, B., Johansen, A.M., Kubilay, N., Losno, R., Maenhaut, W., Paytan, A., Prospero, J.M., Shank, L.M., Siefert, R.L., 2009. Atmospheric iron deposition: global distribution, variability, and human perturbations. Annu. Rev. Mar. Sci. 1, 245–278. https://doi.org/10.1146/annurev.marine.010908.163727.

Markaki, Z., Oikonomou, K., Koçak, M., Kouvrakis, G., Chaniotaki, A., Kubilay, N., Mihalopoulos, N., 2003. Atmospheric deposition of inorganic phosphorus in the Levantine Basin, Eastern Mediterranean: spatial and temporal variability and its role in seawater productivity. Limnol. Oceanogr. 48, 1557–1568.

Markaki, Z., Löye-Pilot, M.D., Violaki, K., Benyahya, L., Mihalopoulos, N., 2010. Variability of atmospheric deposition of dissolved nitrogen and phosphorus in the Mediterranean and possible link to the anomalous seawater N/P ratio. Mar. Chem. 120, 187–194.

Millero, F.J., Feistel, R., Wright, D.G., McDougall, T.J., 2008. The composition of standard seawater and the definition of the reference-composition salinity scale. Deep-Sea Res. Pt. I 55, 50–72. https://doi.org/10.1016/j.dsr.2007.10.001.

Morales-Baquero, R., Pulido-Villena, E., Reche, I., 2006. Atmospheric inputs of phosphorus and nitrogen to the Southwest Mediterranean region: biogeochemical responses of high mountain lakes. Limnol. Oceanogr. 51, 830–837.

Morales-Baquero, R., Pulido-Villena, E., Reche, I., 2013. Chemical signature of Saharan dust on dry and wet atmospheric deposition in the South-Western Mediterranean region. Tellus B: Chemical and Physical Meteorology 65, 18720.

Pey, J., Querol, X., Alastuey, A., Forastiere, F., Stafoggia, M., 2013a. African dust outbreaks over the Mediterranean Basin during 2001–2011: PM10 concentrations, phenomenology and trends, and its relation with synoptic and mesoscale meteorology. Atmos. Chem. Phys. 13, 1395–1410. https://doi.org/10.5194/acp-13-1395-2013.

Pey, J., Pérez, N., Cortés, J., Alastuey, A., Querol, X., 2013b. Chemical fingerprint and impact of shipping emissions over a western Mediterranean metropolis: primary and aged contributions. Sci. Total Environ. 463-464, 497–507. https://doi.org/10.1016/j.scitotenv.2013.06.061.

Prospero, J.M., Barrett, K., Church, T., Dentener, F., Duce, R.A., Galloway II, J.N. Levy, Moody, H., J. and Quinn, P., 1996. Atmospheric deposition of nutrients to the North Atlantic Basin. Biogeochemistry 35, 27–73.

Qu, B., Ming, J., Kang, S.-C., Zhang, G.-S., Li, Y.-W., Li, C.-D., Zhao, S.-Y., Ji, Z.-M., Cao, J.-J., 2014. The decreasing albedo of the Zhadang glacier on western Nyainqentanglha and the role of light-absorbing impurities. Atmos. Chem. Phys. 14, 11117–11128. https://doi.org/10.5194/acp-14-11117-2014.

Rodriguez-Navarro, C., di Lorenzo, F., Elert, K., 2018. Mineralogy and physicochemical features of Saharan dust wet deposited in the Iberian Peninsula during an extreme red rain event. Atmos. Chem. Phys. 18, 10089–10122.

Salvany, J.M., García-Veigas, J., Ortí, F., 2007. Glauberite–halite association of the Zaragoza Gypsum Formation (Lower Miocene, Ebro Basin, NE Spain). Sedimentology 54, 443–467. https://doi.org/10.1111/j.1365-3091.2006.00844.x.

Sánchez-España, J., Mata, M.P., Vegas, J., Morellón, M., Rodríguez, J.A., Salazar, A., Yusta, I., Chaos, A., Pérez-Martínez, C., Navas, A., 2017. Anthropogenic and climatic factors enhancing hypolimnetic anoxia in a temperate mountain lake. J. Hydrol. 555, 832–850. https://doi.org/10.1016/j.jhydrol.2017.10.049.

Seinfeld, J.H., Pandis, S.N., 2006. Atmospheric Chemistry and Physics: From Air Pollution to Climate Change. 2nd edition. John Wiley & Sons, New York.

Torres-Sánchez, R., Sánchez-Rodas, D., Sánchez de la Campa, A.M., Kandler, K., Schneiders, K., de la Rosa, J.D., 2019. Geochemistry and source contribution of fugitive phosphogypsum particles in Huelva, (SW Spain). Atmos. Res. 230, 104650.

Vincent, J., Laurent, B., Losno, R., Bon Nguyen, E., Roullet, P., Sauvage, S., Chevaillier, S., Coddeville, P., Ouboulmane, N., di Sarra, A.G., Tovar-Sánchez, A., Sferlazzo, D., Massanet, A., Triquet, S., Morales Baquero, R., Fornier, M., Coursier, C., Desboeufs, K., Dulac, F., Bergametti, G., 2016. Variability of mineral dust deposition in the western Mediterranean basin and south-east of France. Atmos. Chem. Phys. 16, 8749–8766. https://doi.org/10.5194/acp-16-8749-2016.

Vivanco, M.G., Theobald, M.R., García-Gómez, H., Garrido, J.L., Prank, M., Aas, W., Adani, M., Alyuz, U., Andersson, C., Bellasio, R., Bessagnet, B., Bianconi, R., Bieser, J., Brandt, J., Briganti, G., Cappelletti, A., Curci, G., Christensen, J.H., Colette, A., Couvidat, F., Cuvelier, C., D' Isidoro, M., Flemming, J., Fraser, A., Geels, C., Hansen, K.M., Hogrefe, C., Im, U., Jorba, O., Kitwiroon, N., Manders, A., Mircea, M., Otero, N., Pay, M.-T., Pozzoli, L., Solazzo, E., Tsyro, S., Unal, A., Wind, P., Galmarini, S., 2018. Modeled deposition of nitrogen and sulfur in Europe estimated by 14 air quality model systems: evaluation, effects of changes in emissions and implications for habitat protection. Atmos. Chem. Phys. 18, 10199–10218. https://doi.org/10.5194/acp-18-10199-2018.

Wang, R., Balkanski, Y., Boucher, O., Ciais, P., Peñuelas, J., Tao, S., 2015. Significant contribution of combustion-related emissions to the atmospheric phosphorus budget. Nat. Geosci. 8, 48–54. https://doi.org/10.1038/NGEO2324.

Westrich, J.R., Ebling, A.M., Landing, W.M., Joyner, J.L., Kemp, K.M., Griffin, D.W., Lipp, E.K., 2016. Saharan dust nutrients promote Vibrio bloom formation in marine surface waters. P. Natl. Acad. Sci. 113, 5964–5969. https://doi.org/10.1073/pnas.1518080113.

Yu, H., Chin, M., Yuan, T., Bian, H., Remer, L.A., Prospero, J.M., Omar, A., Winker, D., Yang, Y., Zhang, Y., Zhang, Z., Zhao, C., 2015. The fertilizing role of African dust in the Amazon rainforest: a first multiyear assessment based on data from cloud-aerosol Lidar and infrared pathfinder satellite observations. Geophys. Res. Lett. 42, 1984–1991. https://doi.org/10.1002/2015GL063040.

Zhu, X.R., Prospero, J.M., Millero, J.F., 1997. Diel variability of soluble Fe(II) and soluble total Fe in North African dust in the trade winds at Barbados. J. Geophys. Res.-Atmos. 1022, 21297–21306. https://doi.org/10.1029/97JD01313.